Title
Determining size-specific emission factors for environmental tobacco smoke particles

Journal
Aerosol Science and Technology, 37(10)

ISSN
0278-6826

Authors
Klepeis, N E
Apte, M G
Gundel, L A
et al.

Publication Date
2003-10-01

Peer reviewed

27-March-2003

Determining Size-Specific Emission Factors for Environmental Tobacco Smoke Particles

Neil E. Klepeis,[a,b,*] Michael G. Apte,[b] Lara A. Gundel,[b]
Richard G. Sextro,[b] and William W. Nazaroff [b,c]

[a]Environmental Health Sciences, School of Public Health
University of California at Berkeley
Berkeley, CA 94720

[b]Indoor Environment Department
Lawrence Berkeley National Laboratory
One Cyclotron Road, MS 90-3058
Berkeley, CA 94720

[c]Department of Civil and Environmental Engineering
University of California at Berkeley
Berkeley, CA 94720

Final Revised Version Sent to *Aerosol Science and Technology*

[*]Please address correspondence to Neil E. Klepeis, 16475 Tarpey Road, Watsonville, CA 95076-9015. Email: nklepeis@uclink.berkeley.edu

Abstract

Because size is a major controlling factor for indoor airborne particle behavior, human particle exposure assessments will benefit from improved knowledge of size-specific particle emissions. We report a method of inferring size-specific mass emission factors for indoor sources that makes use of an indoor aerosol dynamics model, measured particle concentration time series data, and an optimization routine. This approach provides – in addition to estimates of the emissions size distribution and integrated emission factors – estimates of deposition rate, an enhanced understanding of particle dynamics, and information about model performance. We applied the method to size-specific environmental tobacco smoke (ETS) particle concentrations measured every minute with an 8-channel optical particle counter (PMS-LASAIR; $0.1-2+$ μm diameters) and every 10 or 30 min with a 34-channel differential mobility particle sizer (TSI-DMPS; $0.01-1+$ μm diameters) after a single cigarette or cigar was machine-smoked inside a low air-exchange-rate 20 m^3 chamber. The aerosol dynamics model provided good fits to observed concentrations when using optimized values of mass emission rate and deposition rate for each particle size range as input. Small discrepancies observed in the first $1-2$ hours after smoking are likely due to the effect of particle evaporation, a process neglected by the model. Size-specific ETS particle emission factors were fit with log-normal distributions, yielding an average mass median diameter of 0.2 μm and an average geometric standard deviation of 2.3 with no systematic differences between cigars and cigarettes. The equivalent total particle emission rate, obtained by integrating each size distribution, was $0.2-0.7$ mg/min for cigars and $0.7-0.9$ mg/min for cigarettes.

Key Words: aerosol dynamics model, cigars, cigarettes, environmental tobacco smoke, exposure assessment, indoor air quality, particle emissions

Running Title: "Size-Specific ETS Particle Emissions"

1 Introduction

Accurate modeling of indoor particle concentrations can improve our understanding of human exposure to particles, including the regional deposition of particles in the lung. To this end, one seeks an improved characterization of the particle size distribution of emissions and a better understanding of indoor particle dynamics. The case of environmental tobacco smoke (ETS) is especially important because of its ubiquity and its implication in adverse health outcomes such as asthma and lung cancer (U.S. EPA 1992).

We are interested here in characterizing "ETS emissions" as opposed to fresh mainstream or sidestream tobacco smoke emissions. Sidestream tobacco smoke is defined as the undiluted plume coming from the smoldering end of the cigarette, and mainstream smoke is the undiluted puff of smoke that is drawn through the cigar or cigarette and then exhaled by the smoker (either a human or a machine). The particles in real or simulated ETS are derived from particles in fresh mainstream and sidestream smoke, but they are different in that they have undergone mixing and dilution (i.e., dispersion) over varying time scales and in a particular indoor setting (e.g., a home, an automobile, or a workplace). While undergoing dispersion, the median tobacco smoke particle size can shrink as particle mass evaporates (Hinds 1978) or it can grow as particles coagulate. The end result can be ETS particle size distributions that are different from the distributions of fresh mainstream or sidestream smoke.

In this study, we aim to determine "effective" ETS emissions, defined as the mass of particles that have come to be dispersed in a previously pollutant-free room just after a cigarette (or cigar) has been smoked. Although several previous investigators have studied tobacco smoke particle size distributions (e.g., Keith and Derrick 1960; Chang et al. 1985; Ueno and Peters 1986; and Chung and Dunn-Rankin 1996), these studies have mostly been focused on mainstream or sidestream smoke, rather than ETS. Those few investigators that have studied ETS particles directly have tended to provide only a cursory examination of the particle size distribution at a particular moment in time (e.g., Benner et al. 1989 and Kleeman et al. 1999).

Therefore, in the present research we seek to provide additional information on size-specific ETS emission factors as well as verified methods for estimating and understanding the time-varying size

distribution of ETS particles. We use a mathematical aerosol dynamics model (Nazaroff and Cass 1989) to interpret measured time-dependent ETS concentrations and to find best estimates of the size-specific particle mass emission rate and particle deposition rate. Our approach is similar to a preliminary effort by Sextro et al. (1991). Since this approach results in estimates of critical parameter values and provides insight into the time scales of particle transformation processes, it will help to facilitate the accurate modeling of tobacco-related indoor particle concentrations and, therefore, the assessment of ETS exposure for both individuals and populations.

In the first section below, we describe our research methods including the chamber experiments, the processing of the observed data, the model, and our procedure for estimating ETS particle mass emissions. The remaining sections present our results, discuss them in light of previous work, and offer some concluding remarks.

2 Methods

2.1 Chamber Experiments

We conducted nine cigar (premium, regular, and cigarillo) and four cigarette (regular and lights) smoking experiments in an unventilated 20 m^3 chamber (see Figure 1 for a schematic). For eight of these experiments, we obtained valid measurements of the particle number concentration (counts per cm^3) in the chamber air every minute using an optical particle counter (LASAIR; Particle Measurement Systems, Inc., Boulder, CO), which registered particle counts in 8 size bins ranging from 0.1 to over 2 μm based on the scattering of 633 nm light emitted from a HeNe laser. The LASAIR input air stream was diluted with filtered air at 5 to 6 times the sample airflow rate. We also measured particle number concentration semi-continuously using a differential mobility particle sizer (DMPS; TSI, Inc., St. Paul, MN), which scanned and sized particles in 34 size bins ranging from approximately 0.01 to over 1 μm in diameter over approximately 10 or 30-minute intervals based on the mobility of charged particles in an electric field. The particle size measurement devices were placed outside the chamber and their input air was drawn through sampling tubes located at a fixed location near the top of the chamber door and more than a foot away from the chamber wall.

During most of the experiments, we made electrochemical measurements of carbon monoxide (CO) every minute using a Langan CO Personal Measurer (Langan Products, San Francisco, CA), which was placed inside the chamber and connected to a Langan DataBear™ digital logger. The CO measurements were used to obtain air exchange rate values for the chamber, which ranged from 0.03 to 0.1 h^{-1}, by fitting a line to the natural logarithm of the decaying CO concentrations. **[During air sampling, unreturned sample flow rates for external instrumentation contributed as much as 0.06 h^{-1} to the overall chamber air exchange rate, an amount comparable to or exceeding the loss from natural leakage.]**

The interior surfaces of the smoking chamber consisted entirely of stainless steel. In addition, two 4-foot by 8-foot sheets of upright gypsum wallboard (a total of approximately 12 m^2 of exposed surface area) were placed vertically in the center of the chamber. **[The wallboard likely caused enhanced deposition of particles and sorption of semivolatile organic chemicals (SVOCs) in the chamber.]** The inside volume of the chamber was approximately 20 m^3 and the surface area was approximately 57 m^2 – including the wallboard – giving a surface-to-volume ratio of 2.9 m^{-1}.

We smoked pre-weighed cigars and cigarettes using a smoking machine (ADL/II, Arthur D. Little, Inc., Cambridge, MA) at the standard rate of two 35-cm^3 puffs per minute. The cigars were 13-cm regular Swisher Sweets, aromatic and mild blend plastic-tipped Tiparillos (cigarillos), and an 18-cm Macanudo premium. The cigarettes were Camel lights and Marlboro regulars.

An investigator ignited the tobacco products using a hand lighter, whereupon he exited the chamber and securely closed the airtight door. Both sidestream and mainstream tobacco smoke were freely emitted into the chamber where they were thoroughly mixed by six small fans – two aimed up at the plume with four more cycling air clockwise around the chamber. **[The fans raised the air velocity in the chamber to a level somewhat above those that might exist in a quiescent residential location.] [For each experiment, a single cigarette was held in place by a custom-designed automatic smoking carousel connected to the smoking machine, while each cigar was attached to a nearby stand and connected to the smoking machine using a copper fitting, Teflon tape, and plastic tubing.]** During smoking, we observed through the chamber window that the smoke plumes became

rapidly dispersed over a period of a few seconds, **[suggesting that emissions were thoroughly mixed throughout the chamber volume within a very short time period]**.

We used a timer to disconnect power from the smoking machine after a preset smoking time ($10-15$ min for cigars and $5-8$ min for cigarettes). The smoldering cigars and cigarettes were rapidly extinguished from outside of the closed chamber by forcing nitrogen gas in reverse direction through the cigarette or cigar.

Once the sources were completely extinguished, we began collecting total particle mass (TPM) on Teflon-coated glass fiber filters **[with no size selection]**, sampling at approximately 18 liters/min over time periods ranging from 30 to 60 min. The LASAIR and DMPS, being activated before the sources were ignited to measure background levels, were left to record particle number concentrations in the sealed chamber for at least 12 hours and, in some cases, up to 24 hours after smoking. We found the background levels to be negligible compared to the peak concentrations in each experiment for each particle size range.

We determined TPM concentration gravimetrically by weighing the accumulated mass on each filter with a Cahn-25 precision electrobalance and dividing it by the volume of chamber air sampled. The filters were frozen following each experiment, and then thawed and equilibrated to ambient relative humidity prior to being reweighed. The TPM emitted by a cigar or cigarette during each experiment was estimated from the filter TPM concentrations by taking into account the loss of mass from deposition and ventilation that occurred during sample collection. We estimated the total particle removal rate for each experiment by fitting a line to the logarithm of the decaying total particle counts as measured by the LASAIR. On the day following each experiment, the unsmoked portion of each cigar or cigarette was weighed to determine the mass of tobacco that had been consumed by smoking. **[TPM concentrations measured just after smoking ranged from 180 to 560 μg m^{-3}, averaging 370 μg m^{-3}. These levels are typical of those that might occur in a smoking lounge or other indoor location where smoking is allowed.]**

2.2 Determining Size Characteristics

2.2.1 Processing the Data

To estimate the mass of ETS particles emitted in each size range, we analyzed particle count data measured with the LASAIR and DMPS instruments. We converted the LASAIR- and DMPS-measured particle number concentrations to particle mass concentrations for each particle size range by assuming that ETS particles have a density of 1.1 g/cm^3 (Lipowicz 1988), that the logarithm of the particle mass concentration is uniformly distributed within each size range, and that ETS particles are spherical.

The LASAIR was originally calibrated with latex spheres, which have a different refractive index (1.588 - 0i) than ETS particles (1.532 + 0i; McRae 1982). We post-calibrated the LASAIR data by comparing the calculated LASAIR response for ETS particles to those for latex spheres (Bohren and Huffman 1983; Garvey and Pinnick 1983).

Sufficiently high quality data from the DMPS were limited to three of the cigar experiments and these data did not, in general, possess high time resolution or uniformity since each scan lasted from 10 to 30 min and there was sometimes a delay between scans. Therefore, with regard to the optimization procedure, the use of the DMPS data was limited to providing initial estimates of the proportion of mass emitted for particles smaller than 0.1 μm, a diameter range not sampled by the LASAIR.

For the parameter optimization procedure described below, we estimated initial particle emissions independently for each size range using the following formula:

$$E = \phi V \overline{C} + \frac{V}{T_{off} - T_{on}} C_{peak} \tag{1}$$

where E is the mass emission rate for each bin [μg/min], ϕ is the total loss rate for each bin [min^{-1}], V is the chamber volume [m^3], C_{peak} is the peak particle concentration for each size range above a zero background [μg m^{-3}], and $\overline{C}$ is the average concentration [μg m^{-3}] between the time the source started, T_{on} [min], and the time the source ended, T_{off} [min]. $\overline{C}$ was approximated as $\frac{C_{peak}}{2}$. The loss rate ϕ for each particle diameter range was estimated by fitting a line to the logarithm of the decaying

concentrations.

2.2.2 Modeling Aerosol Dynamics

We adapted the aerosol dynamics model of Nazaroff and Cass (1989) to calculate ETS particle concentrations for each experiment, taking into account the effects of ventilation, particle coagulation, deposition, and direct emissions from a cigar or a cigarette. Coagulation, deposition, and emission change the size distribution of airborne particles. In contrast, ventilation removes particles at an equal rate across all sizes.

Although creation of new particle mass can occur through condensation of semi-volatile organic compounds (SVOCs) from particles, we do not expect this process to play an important role in ETS aerosol dynamics. Kousaka et al. (1982) report that humidity only affects the growth of smoke particle size under supersaturated conditions, which do not apply in our case. The shrinkage of particles owing to SVOC evaporation can also occur for ETS, such as when rapid mixing and dilution occur after smoking. Both Ingebrethsen and Sears (1989) and Hinds (1978) provide evidence of this phenomenon.

2.2.3 Optimizing Model Parameters

For experiments in the current study, we have knowledge of the chamber ventilation rate and source duration, and the rate of particle coagulation is calculated based on concentrations occurring in a given time step. The two remaining, unknown model parameters are the magnitude of the particle mass emissions and the rate of particle deposition onto surfaces. We refer to mass emissions in terms of three types of emission factors: the mass emission rate (mg emitted per minute); the total particle mass (TPM) emissions (mg emitted per tobacco source); and the mass-normalized emissions (mg emitted per gram of tobacco consumed).

Our task is to find values of the unknown model parameters for each particle size range (or bin) that result in the best fit of model predictions to measured concentrations. In addition to tuning model input values, the fits also provide an indication of model accuracy. We used the following steps

to obtain optimal values of mass emissions and deposition loss-rate coefficient for each measured particle diameter from each of the eight chamber experiments in which valid LASAIR measurements were recorded.

Step 1. From the LASAIR data, we made initial guesses of the mass emission rate and deposition loss-rate coefficient for each optimization from observed peak concentrations and decay rates for each size bin, assuming independence among the bins (see Equation 1). The initial guess for deposition loss rate was calculated by subtracting the ventilation rate from the overall particle loss rate. These initial values are expected to be in error since the loss or gain of particle mass in each bin depends on coagulation.

Step 2. We used the aerosol dynamics model and a local grid search routine to locate the optimal values of mass emission rate and deposition rate for each particle size range starting at 0.1 μm, which is the lower limit for the LASAIR, and ending at the bin with a 2.0 μm lower limit. For the goodness-of-fit statistic between modeled and observed mass concentration time series, we used the mean absolute deviation, which is less sensitive to outliers than the mean squared deviation. A time period of 8 hours was selected for each experiment, since it would capture time-dependent dynamics over a relatively long time scale but avoid appreciable shifts in background concentration that appeared to occur over $12-24$ h time periods. The sample size of each series used in the optimization was approximately 400 for each experiment. The optimization surface was generally smooth with a clear minimum, as illustrated for the $0.1-0.2$ μm particle diameter range in the *top panel* of Figure 2. The *bottom panel* of Figure 2 contains an illustration of the grid search method for the same experiment and size range. Since emissions in each bin can influence concentrations in adjacent bins through coagulation, we repeated the optimization, using the final values from one run as the starting values for the next run, until the starting values remained unchanged for all size bins.

Step 3. Using the above steps and the DMPS data from three cigar experiments, where the DMPS scan times were 10 min or less, we obtained size-specific mass emission and deposition rates in twelve aggregated size ranges from about 0.009 to 1.154 μm. This range appeared to encompass most of the particle sizes present in ETS. Each of the three experiments showed that about 20% of

the emitted particle mass was smaller than 0.1 μm. The lower end of observed ETS particle sizes was $0.02-0.03$ μm.

Step 4. The LASAIR-based optimization (step 2) was repeated using initial guesses from the results of step 3 for particles smaller than 0.1 μm. The emissions and deposition rates for particles smaller than 0.1 μm were optimized by calculating the mean absolute deviation between observed and predicted concentrations across all larger sizes. Initial guesses for the other size ranges (> 0.1μm) were obtained from the ending values in step 2. As in step 2, we repeated the overall optimization process (from lowest to hightest bin) until the parameter values remained unchanged. The surface for the "indirect" optimization of emissions smaller than 0.1 μm was irregular and much flatter than for other particle sizes, indicating more uncertainty.

Step 5. After the optimization procedure was completed for each experiment, we fit a log-normal distribution to the optimized mass emission rate to obtain estimates for the mass median diameter (MMD) and geometric standard deviation (GSD) of the emissions size distribution. These fitted parameters are the same whether for the distribution of TPM emissions (mg), mass emission rate (mg/min), or mass-normalized emissions (mg/g-smoked).

Step 6. To estimate uncertainty in the log-normal size distribution parameters, we repeated steps $2-5$ for slightly perturbed initial values in each size range, including particles smaller than 0.1 μm. Owing to the large computational time required for a single optimization, it was impractical to conduct a large number of optimization trials. A comparison of final optimization results to initial values provides an approximate characterization of uncertainty.

3 Results and Discussion

3.1 Model Performance

The fits between LASAIR-observed and modeled time series data were generally good with minima for the mean absolute deviation in each bin ranging from 0.4 to 3 μg m^{-3}. Figure 3 shows an example optimal fit of a modeled times series to an observed times series for four particle diameter ranges. For bins between 0.1 and 1 μm, the error across all experiments was between 2 and 12%.

A linear regression of predicted time series values (dependent variable) against the observed values (independent variable) for these bins yielded coefficients of determination, i.e., r^2 values, between 0.8 and 1 across all experiments, except for the $0.3-0.4$ μm particle size range in two experiments where r^2 values were 0.6 and 0.7.

We observed small systematic deviations in the fits at the beginning of a few time series, where the observed particle loss appeared to be faster than later in the time series. This "early decay" effect may be due to evaporative losses as suggested by Ingebrethsen and Sears (1989) and Hinds (1978). Figure 4 shows an example optimal fit for which particles in the $0.3-0.4$ μm particle diameter range appear to undergo evaporation during the first $1-2$ hours after smoking stopped – a behavior that does not appear to be well-captured by the model. Incomplete mixing is unlikely to explain the early decay, since not all size ranges exhibited this behavior for a given experiment (e.g., the $0.2-0.3$ μm diameter range in Figure 4).

The model seemed to accurately account for the effect of particle coagulation, which influenced concentrations in the smaller size bins for times as long as 4 hours after the source was extinguished. Second-order coagulation processes caused the concentrations for the lower diameter ranges to actually increase after the source was extinguished. This behavior is captured by the model and occurs as emissions in smaller size ranges transfer particle mass into larger size ranges.

3.2 Estimates of the ETS Particle Size Distribution

Table 1 contains best estimates of the ETS particle mass emissions size distribution, based on the LASAIR data collected during eight experiments. Figure 5 presents the log-normal fits to the optimization results of each experiment. The MMD's for the emissions are close to particle diameters of 0.2 μm for all source types ($\overline{x}$ = 0.20; s = 0.017; COV = 8%), with the GSD's ranging from 1.9 to 3.1 ($\overline{x}$ = 2.3; s = 0.37; COV = 16%). ETS particle emissions appear to be due mostly to particles that have diameters between 0.02 and 2 μm – with no clear difference in the estimated mass size distributions between cigars and cigarettes.

The uncertainty in our LASAIR-based estimates is highest for particles smaller than 0.1 μm, since

they are based on an indirect fitting procedure. However, after repeating the procedure for each experiment for different starting points, the fitted MMD and GSD were 0.16$-$0.23 μm and 1.9$-$3.1, respectively. These represent differences of 0$-$13% in MMD and 2$-$10% in GSD from the values in Table 1. These differences are comparable to the coefficient of variation (COV) across all experiments and source types for the final results stated above. In other words, parameter uncertainty appears to be on the order of parameter variability. In contrast, our initial guess for the size distribution, which (using the LASAIR data and assuming independence between bins) did not consider coagulation or particle mass below 0.1 μm, had MMD's and GSD's that ranged from 0.22$-$0.30 μm and 1.4$-$2.1, respectively – differences of 14$-$39% and 10$-$34% when compared to our final results. The MMD's are higher and the GSD's are smaller (i.e., the distribution is more narrow) than for our final estimates, because of the neglected particle mass. These differences give an indication of the maximum error one would expect when using the raw LASAIR data to directly estimate ETS particle emissions characteristics.

Since our approach neglects evaporation, our results may be influenced by the evaporation of SVOC particle constituents. The true emissions may be larger in magnitude and occur at larger particle sizes than we determined. However, using the optimal values of emissions and deposition rate for input, our model provides a good fit to ETS particle concentrations for most size ranges and for most times (with model errors generally near or below 10% for 0.1 - 1 μm particles), and we therefore judge it to be an appropriate tool for predicting concentrations and exposures. The agreement between our model and the observed concentrations suggests that the evaporation of SVOCs from ETS particles may not be a very large effect.

The optimized DMPS particle mass emissions distributions, which were used to give initial estimates for particle sizes smaller than 0.1 μm during the LASAIR-based optimization procedure, all had MMD's of 0.20$-$0.22 μm with geometric standard deviations of 1.81$-$1.86. See Figure 6 for a sample fitted log-normal distribution for DMPS data. The GSD values, which are lower than our final LASAIR-derived values, may be due to a small amount of neglected mass greater than 1 μm in diameter. Also, the largest size ranges measured by the LASAIR and DMPS have more uncertainty

associated with them than the middle size ranges.

Based on optimization, approximately 20% of the DMPS particle mass was found to be emitted for sizes smaller than 0.1 μm for each of the experiments. To compare these results to a direct estimate from the DMPS data alone (i.e., without applying the model-based optimization procedure), we fit a log-normal distribution to the measured particle number size distribution from the DMPS data that was collected just after the cigar or cigarette was extinguished. The resulting count median diameters (CMD's) were $0.07-0.09$ μm and geometric standard deviations were all near 1.8 with a corresponding mass median diameter (MMD) of $0.20-0.25$ μm (Hinds 1982). These values for MMD and GSD, which neglect particle transformation processes that may have occurred in the first few minutes after the smoke was mixed, are reasonably close to the estimates obtained by using the optimization procedure. These results provide a measure of self-consistency in our approach, and they support the practice of using sufficiently time-resolved concentration measurements by themselves to provide estimates of size-specific ETS emissions.

3.2.1 Other Studies of Size-Specific Emissions

Our results for the size distribution of ETS particle emissions are in generally good agreement with the findings of other investigators who, although they may not have examined ETS *per se*, have studied mainstream or sidestream smoke, typically after it has been aged and/or diluted. Because concentrated tobacco smoke undergoes coagulation and, in addition, evaporation can occur during dilution, the size distribution of the smoke is sensitive to experimental conditions. Therefore, investigations of fresh or diluted-and-aged mainstream or sidestream smoke are not likely to give results identical to ours. In addition, most of these investigations have used a non-model-based approach to estimate the emissions size distribution.

MMD values reported in the literature are in the approximate range of $0.3-0.7$ μm for mainstream smoke (Chang et al. 1985; Anderson et al. 1989; and Chung and Dunn-Rankin 1996), $0.2-0.5$ μm for sidestream smoke (Ueno and Peters 1986; Ingebrethsen and Sears 1989; and Chung and Dunn-Rankin 1996), and $0.2-0.5$ μm for ETS (Benner et al. 1989; Sextro et al. 1991 as reported in Nazaroff

et al. 1993; Kleeman et al. 1999), with reported GSD values in the approximate range of $1-2$. In spite of the variation in these reported results, ETS particle emissions appear to have a fairly narrow and identifiable distribution. Nearly all freshly dispersed ETS particle mass lies in the diameter range of $0.02-2$ μm.

3.3 Estimates of Size-Integrated Emission Factors

Table 2 contains a summary of each experiment and the filter-based results for size-integrated mass emission rates, mass-normalized emissions, and total particle mass (TPM) emissions. Equivalent TPM emissions determined by integrating the particle mass size distributions (Table 1) were generally lower than those determined using filters (Table 2) with total particle mass emissions that were $54-84$% of the filter-based emissions (absolute differences were $0.9-4.3$ mg per cigarette or cigar). **[Large non-ETS particles, such as resuspended dust, may have contributed to the larger TPM values for filters, although low observed background levels make this possibility seem unlikely.]** Instead, the larger TPM values for filters may be a consequence of the collection onto the filters, by sorption or condensation, of SVOCs present in ETS **[in quantities greater than for the competing effect of particle mass evaporation, which might have occurred either during or after sample collection.]** Since vapor-phase compounds are likely not detected by the real-time particle sizing instrumentation, sorption of nicotine and other SVOCs onto filters could have contributed to the observed discrepancies (Mader and Pankow 2001). Daisey et al. (1998) report sidestream nicotine emission factors of $5-7$ mg per cigarette.

The equivalent integrated emissions were consistently higher for cigarettes ($7-8$ mg/g-smoked and $0.7-0.9$ mg/min) than for cigars ($3-5$ mg/g-smoked and $0.2-0.7$ mg/min). The total particle mass emitted by the cigarillos and premium cigar and their emission rates were markedly lower than for the other types of cigars and for cigarettes, although this finding may be an artifact of leakage around the end-fittings during smoking (the cigarillos had plastic tips and the premium cigar was rather bulky). The mass-normalized emissions (mg/g-smoked), which may be more appropriate for direct comparisons, showed consistent results among different types of cigars.

As a side note, the total mass-normalized CO emissions determined from real-time CO measurements in our study ranged from 62 to 122 mg/g-smoked for 6 cigars, 139 to 162 mg/g-smoked for 3 cigarillos, and 102 to 226 mg/g-smoked for 3 cigarettes. Klepeis et al. (1999) report an average of 155 mg/g-smoked for 10 different cigars with a range of 82 to 200 mg/g-smoked, values which are comparable to our results.

3.3.1 Other Studies of Integrated Mass Emissions

In alignment with our study, Ueno and Peters (1986) and Chang et al. (1985) report equivalent total mass emissions from real-time instruments (using an electrical mobility analyzer and condensation nucleii counter) that are substantially smaller than determinations based on direct mass measurements (a cascade impactor in their case). Chang et al. (1985) found that when their primary dilution ratio for mainstream smoke was increased from 6 to 18, the equivalent TPM measured from their electrical mobility analyzer decreased dramatically (18 mg/cigarette down to 2.0 mg/cigarette) while the TPM measured with the cascade impactor remained approximately the same (19−21 mg/cigarette). For sidestream smoke, Ueno and Peters (1986) report cascade impactor TPM measurements of 6.0−9.6 mg/cigarette across all primary dilution ratios (6−18) compared to equivalent TPM from the electrical mobility analyzer of 1.3−2.3 mg/cigarette. As far as we know, these discrepancies have not been resolved and will require further investigation.

The gravimetrically-determined values for ETS particle emission factors reported in the literature are in the approximate range of 8−20 mg per cigarette smoked (see Hammond et al. 1987; Eatough et al. 1989; Löfroth et al. 1989; Hildemann et al. 1991; Leaderer and Hammond 1991; Koutrakis et al. 1992; Özkaynak et al. 1996; Martin et al. 1997; and Daisey et al. 1998) and approximately 6−50 mg/g-smoked for cigars (see CPRT Laboratories 1990 as reported in NCI 1998; Leaderer and Hammond 1991; Nelson et al. 1998; Nelson et al. 1999; and Klepeis et al. 1999). These ranges indicate substantial amounts of unexplained variability, probably stemming from different experimental conditions and methodologies (e.g., sampling volume) in addition to the variety of tobacco products that were used.

3.4 Estimates of Particle Deposition Loss

Figure 7 presents our estimates of the deposition loss-rate coefficient in h^{-1} across six particle diameter ranges and corresponding to the eight experiments in Table 1. Our results for the lowest and highest diameter ranges were most uncertain because of either an indirect optimization approach ($0.02-0.1$ μm) or measurement scatter from sparse particle counts ($1-2$ μm). Also in Figure 7 are deposition loss-rate coefficients determined by Xu et al. (1994) in chamber experiments where four small wall fans were operated over a range of different speeds. Their results for the case of the maximum fan speed of 3070 rpm, which is similar to the speed of the six wall fans used in our own experiments, are shown. For particles between 0.1 and 1 μm, which is the range of highest certainty for our own results, there is fairly good agreement between the two studies.

4 Summary and Conclusions

In this paper, we present a model-based method for estimating size-specific particle mass emission factors for indoor sources, and the results of applying this method to data from a set of cigar and cigarette chamber experiments. The method hinges on an iterative optimization procedure, which minimizes the difference between predicted and observed time series as a function of size-specific emission rate and deposition loss rate. Since ETS particle concentrations depend on the conditions of mixing and dilution, including smoking style, which can vary from one smoking situation to another, our method estimates "effective" emissions that result when the raw mainstream and/or sidestream emissions have been dispersed (mixed and diluted) in a room under a specific set of conditions.

The approach is general and can be used to interpret size-specific emissions from other indoor particle sources. It requires a time series of measured particle concentrations over the range of existing particle sizes and collected following a prescribed emission activity. The time series need not be regularly-spaced or include points immediately following release, and it can consist of time-averaged elements over $10-15$ min or more. Measurements should be made with higher time resolution than the dynamics of the system, which is on the order of an hour or less for typical indoor environments.

Some advantages of our approach are that multiple model parameters can be estimated simul-

taneously from the data, features of the observed time series can be explained in terms of specific transformation processes, and we arrive at an emissions-calibrated aerosol dynamics model. This model can then be used to predict the effect of tobacco smoking on size-resolved indoor particle concentrations, and, therefore, in human exposure and risk assessments. The key limitation of the method is that it depends on the accuracy of the model, although this accuracy can be explored as part of the approach.

An alternative technique to estimate ETS emissions (and one used by other investigators) is to measure concentrations immediately after smoking and once mixing is complete. We found this approach to give results similar to those for our optimization approach, although it requires fairly highly resolved measurements in time.

Our approach provided good model fits to data collected in a room-sized chamber. Although our results may implicitly include the evaporation of tobacco smoke particle constituents in the short time between the smoke's release and its dispersion in the study chamber, a process not included in our model, our estimates of the size distribution of particle mass emisions are within the range of observations of other researchers.

As with a few other researchers, we found a discrepancy between total particle mass determined indirectly from size-specific measurements versus those determined directly from filter measurements. Future research should aim to resolve such discrepancies, e.g., by examining the differential collection of semi-volatile organic compounds in tobacco smoke with respect to measurement method.

Additional ETS emissions characterization and model evaluation studies, similar to ours, should be carried out using designed experiments that capture real-world variation in room conditions and smoking behavior. It may be advantageous to develop an explicit module for the aerosol dynamics model that simulates evaporation and condensation. In the interest of improving aerosol human exposure and risk assessments, the size-resolved emissions of other indoor particle combustion sources that emit submicron particles – such as heaters, stoves, incense, or candles – should also be studied.

Acknowledgements

This work was supported in part by the U.S. Environmental Protection Agency (EPA) National Exposure Research Laboratory through Interagency Agreement DW-988-38190-01-0 with the U.S. Department of Energy (DOE) under Contract Grant No. DE-AC03-76SF00098 at Lawrence Berkeley National Laboratory. The experimental work was supported with California Tobacco-Related Disease Research Program (TRDRP) funds under grant 6RT-0307 to Lawrence Berkeley National Laboratory, and by the Assistant Secretary of Conservation and Renewable Energy, Office of Building Technologies, Building Systems and Materials, Division of the U.S. Department of Energy (DOE) under Contract DE-AC03-76SF0098. Additional support was provided by the TRDRP under grant 6RT-0118 to Stanford University. We would like to express our appreciation for the technical assistance of D. Sullivan. S. Baker assisted with filter preparation and experimental procedure. The graphics and much of the data analysis for this research were accomplished using the freely-available R system described by Ihaka and Gentleman (1996) and accessible on the world wide web at `http://www.r-project.org`.

References

Anderson, P.J., J.D. Wilson, and C.F. Hiller. 1989. “Particle Size Distribution of Mainstream Tobacco and Marijuana Smoke.” *American Review of Respiratory Disease* 140:202–205.

Benner, C.L., J.M. Bayona, F.M. Caka, H. Tang, L. Lewis, J. Crawford, J.D. Lamb, M.L. Lee, L.D. Hansen, and D.J. Eatough. 1989. “Chemical Composition of Environmental Tobacco Smoke. 2. Particulate-Phase Compounds.” *Environmental Science and Technology* 23 (6):688–699.

Bohren, C.F, and D.R. Huffman. 1983. *Absorption and Scattering of Light by Small Particles*. New York: John Wiley and Sons.

Chang, P.T., L.K. Peters, and Y. Ueno. 1985. “Particle Size Distribution of Mainstream Cigarette Smoke Undergoing Dilution.” *Aerosol Science and Technology* 4:191–207.

Chung, I., and D. Dunn-Rankin. 1996. “In Situ Light Scattering Measurements of Mainstream and Sidestream Cigarette Smoke.” *Aerosol Science and Technology* 24:85–101.

CPRT Laboratories, Inc. 1990. “Development of Methods for the Characterization of Toxic Constituents in Cigars, Pipe Tobacco, and Smokeless Tobacco.” Technical Report SSSC Contract H4078-1-C230/01-SS, Tobacco Branch, Health Canada. Cited on pp. 169 and 178 of NCI (1998).

Daisey, J.M., K.R.R. Mahanama, and A.T. Hodgson. 1998. “Toxic Volatile Organic Compounds in Simulated Environmental Tobacco Smoke.” *Journal of Exposure Analysis and Environmental Epidemiology* 8(3):313–334.

Eatough, D.J., C.L. Benner, J.M. Bayona, G. Richards, J.D. Lamb, M.L. Lee, E.A. Lewis, and L.D. Hansen. 1989. “Chemical Composition of Environmental Tobacco Smoke. 1. Gas-Phase Acids and Bases.” *Environmental Science and Technology* 23(6):679–687.

Garvey, D.M., and R.G. Pinnick. 1983. “Response Characteristics of the Particle Measurement Systems Active Scattering Aerosol Spectrometer Probe (ASASP-X).” *Aerosol Science and Technology* 2:477–488.

Hammond, S.K., B.P. Leaderer, A.C. Roche, and M. Schenker. 1987. “Collection and Analysis of Nicotine as a Marker for Environmental Tobacco Smoke.” *Atmospheric Environment* 21(2):457–462.

Hildemann, L.M., G.R. Markowski, and G.R. Cass. 1991. “Chemical Composition of Emissions from Urban Sources of Fine Organic Aerosol.” *Environmental Science & Technology* 25(4):744–759.

Hinds, W.C. 1978. “Size Characteristics of Cigarette Smoke.” *American Industrial Hygiene Association Journal* 39:48–54.

Hinds, W.C. 1982. *Aerosol Technology: Properties, Behavior, and Measurement of Airborne Particles*. New York: John Wiley and Sons.

Ihaka, R., and R. Gentleman. 1996. “R: A Language for Data Analysis and Graphics.” *Journal of Computational and Graphical Statistics* 5:299–314.

Ingebrethsen, B.J., and S.B. Sears. 1989. “Particle Evaporation of Sidestream Tobacco Smoke in a Stirred Tank.” *Journal of Colloid and Interface Science* 131(2):526–536.

Keith, C.H., and J.C. Derrick. 1960. “Measurement of the Particle Size Distribution and Concentration of Cigarette Smoke by the "Conifuge".” *Journal of Colloid Science* 15:340–356.

Kleeman, M.J., J.J. Schauer, and G.R. Cass. 1999. "Size and Composition Distribution of Fine Particulate Matter Emitted from Wood Burning, Meat Charbroiling, and Cigarettes." *Environmental Science & Technology* 33(20):3516–3523.

Klepeis, N.E., W.R. Ott, and J.L. Repace. 1999. "The Effect of Cigar Smoking on Indoor Levels of Carbon Monoxide and Particles." *Journal of Exposure Analysis and Environmental Epidemiology* 9(6):622–635.

Kousaka, Y., K. Okuyama, and C. Wang. 1982. "Response of Cigarette Smoke Particles to Change in Humidity." *Journal of Chemical Engineering of Japan* 15(1):75–76.

Koutrakis, P., S.L.K. Briggs, and B.P. Leaderer. 1992. "Source Apportionment of Indoor Aerosols in Suffolk and Onondaga Counties, New-York." *Environmental Science & Technology* 26(3):521–527.

Leaderer, B.P., and S.K. Hammond. 1991. "Evaluation of Vapor Phase Nicotine and Respirable Suspended Particle Mass as Markers for Environmental Tobacco Smoke." *Environmental Science and Technology* 25:770–777.

Lipowicz, P.J. 1988. "Determination of Cigarette Smoke Particle Density from Mass and Mobility Measurements in a Millikan Cell." *Journal of Aerosol Science* 19(5):587–589.

Löfroth, G., R.M. Burton, L. Forehand, S.K. Hammond, R.L. Seila, R.B. Zweidinger, and J. Lewtas. 1989. "Characterization of Environmental Tobacco Smoke." *Environmental Science and Technology* 23(5):610–614.

Mader, B.T., and J.P. Pankow. 2001. "Gas/Solid Partitioning of Semivolatile Organic Compounds (SOCs) to Air Filters. 3. An Analysis of Gas Adsorption Artifacts in Measurements of Atmospheric SOCs and Organic Carbon (OC) When Using Teflon Membrane Filters and Quartz Fiber Filters." *Environmental Science and Technology* 35(17):3422-3432.

Martin, P., D.L. Heavner, P.R. Nelson, K.C. Maiolo, C.H. Risner, P.S. Simmons, W.T. Morgan, and M.W. Ogden. 1997. "Environmental Tobacco Smoke (ETS): A Market Cigarette Study." *Environment International* 23:75–90.

McRae, D.D. 1982. "The Refractive-Index of Individual Cigarette-Smoke Droplets." *Journal of Colloid and Interface Science* 87(1):117–123.

Nazaroff, W.W., W.Y. Hung, A.G. B.M. Sasse, and A.J. Gadgil. 1993. "Predicting Regional Lung Deposition of Environmental Tobacco Smoke Particles." *Aerosol Science and Technology* 19(3):243–254.

Nazaroff, W.W., and G.R. Cass. 1989. "Mathematical Modeling of Indoor Aerosol Dynamics." *Environmental Science and Technology* 23:157–165.

NCI. 1998. *Cigars: Health Effects and Trends*. Bethesda: National Institutes of Health, National Cancer Institute. NIH Publication Number 98-4302.

Nelson, P.R., S.P. Kelly, and F.W. Conrad. 1998. "Cigars as a Source of Environmental Tobacco Smoke." *Journal of Aerosol Science* 29(Suppl 1):S1307–S1308.

Nelson, P.R., S.P. Kelly, R.W. Conrad, J. Richardson, and C.H. Risner. 1999. Characterization of Environmental Tobacco Smoke from Cigars. Proceedings of the 8th International Conference on Indoor Air Quality and Climate – Indoor Air '99. Edinburgh, Scotland.

Özkaynak, H., J. Xue, J. Spengler, L. Wallace, E. Pellizzarri, and P. Jenkins. 1996. "Personal Exposure to Airborne Particle and Metals - Results from the Particle TEAM Study in Riverside, California." *Journal of Exposure Analysis and Environmental Epidemiology* 6(1):57–78.

Sextro, R.G., E. Gross, and W.W. Nazaroff. 1991, October. Determination of Emissions Profiles for Indoor Particle Phase Environmental Tobacco Smoke. Presented at the 1991 Annual Meeting of the American Association for Aerosol Research. Traverse City, MI.

Ueno, Y., and L.K. Peters. 1986. "Size and Generation Rate of Sidestream Cigarette Smoke Particles." *Aerosol Science and Technology* 5:469–476.

U.S. EPA. 1992, December. "Respiratory Health Effects of Passive Smoking: Lung Cancer and Other Disorders." Technical Report EPA/600/6-90/006F, U.S. Environmental Protection Agency, Office of Research and Development, Washington, D.C.

Xu, M.D., M. Nematollahi, R.G. Sextro, A.J. Gadgil, and W.W. Nazaroff. 1994. "Deposition of Tobacco Smoke Particles in a Low Ventilation Room." *Aerosol Science and Technology* 20(2):194–206.

Table 1: The Estimated Size Distributions of ETS Particle Emissions[a]

Experiment[c]	MMD [μm]	GSD	Integrated ETS Particle Emissions[b] TPM [mg]	Rate [mg/min]	Mass-Normalized [mg/g-smoked]
Regular Cigar #1	0.18	2.5	8.8	0.71	5.2
Regular Cigar #2	0.21	2.2	6.7	0.46	4.6
Regular Cigar #3	0.20	2.4	6.3	0.61	3.3
Premium Cigar	0.18	1.9	4.7	0.35	3.7
Cigarillo #2	0.23	3.1	2.8	0.19	2.9
Cigarette #2	0.21	2.1	5.5	0.90	7.6
Cigarette #3	0.20	2.1	5.0	0.68	7.0
Cigarette #4	0.19	2.1	5.1	0.71	7.1

[a]These estimates are based primarily on the LASAIR data with initial guesses for particle mass smaller than 0.1 μm determined from DMPS-based optimization results. The size metric is particle diameter measured in μm. MMD is the fitted mass median diameter of each size distribution and GSD is the fitted geometric standard deviation.

[b]The "integrated" total particle mass (TPM), emission rate, and mass-normalized emissions were obtained by integrating the estimated size distribution of total mass emissions and dividing by unity, the smoking time, or the mass of tobacco consumed, respectively.

[c]Table 2 contains data on smoking time and tobacco mass consumed for each experiment and the results of five additional experiments for which only filter-based, non-size-specific total mass emissions were determined.

Table 2: Summary of Cigar and Cigarette Experiments and Filter-Based ETS Particle Emissions

Experiment	Smoking Duration [min]	Tobacco Mass Consumed [g]	Filter-Based ETS Particle Emissions[a]		
			TPM [mg]	Rate [mg/min]	Mass-Normalized [mg/g-smoked]
Regular Cigar #1	12.5	1.71	10.8	0.86	6.3
Regular Cigar #2	14.8	1.46	8.1	0.55	5.6
Regular Cigar #3	10.3	1.92	9.5	0.92	4.9
Regular Cigar #4	11.3	1.41	11.8	1.04	8.4
Regular Cigar #5	14.0	1.50	7.3	0.52	4.8
Premium Cigar	13.4	1.26	5.6	0.42	4.5
Cigarillo #1	10.1	1.02	4.0	0.67	6.6
Cigarillo #2	14.8	0.96	4.0	0.27	4.1
Cigarillo #3	14.8	1.36	6.3	0.42	4.6
Cigarette #1	5.5	0.73	9.8	1.79	13.4
Cigarette #2	6.1	0.72	7.0	1.15	9.7
Cigarette #3	7.4	0.72	9.3	1.3	13.0
Cigarette #4	7.1	0.72	7.3	1.03	10.1

[a]The total particle mass (TPM) emitted by a cigar or cigarette during each experiment was estimated from filter data by taking into account the loss of mass from deposition and ventilation that occurred during sample collection. We estimated the effective total particle removal rate for each experiment by fitting a line to the logarithm of the decaying total particle counts as measured by the LASAIR. Emission rate and mass-normalized emissions were calculated by dividing the TPM emissions by the smoking time or mass of tobacco consumed, respectively.

Figure Captions

Figure 1. A schematic of the experimental chamber showing the chamber dimensions and the approximate placement of the sampling tubes, cigar and cigarette sources, CO monitor, two sheets of wallboard, and six mixing fans. The surface-to-volume ratio of the chamber, including the two sheets of upright wallboard, was 2.9 m^{-1}. The particle sampling tubes were connected to particle sizing instrumentation based on either light-scattering (LASAIR) or electrostatic mobility (DMPS).

Figure 2. The top panel shows contours of an optimization surface for particles with diameters of $0.1-0.2$ μm (for the *Cigarillo #2* experiment) over a range of emission rates and deposition rates. The bottom panel depicts an optimization pathway, illustrating how a local grid search method was used to find the minimum point on the surface and the optimal values of model input parameters, here 0.125 h^{-1} for deposition loss-rate coefficient and 50 μg/min for emission rate. The circle size is proportional to the mean absolute deviation between elements of the observed and modeled time series, indicating the error of the model in fitting the measurements at particular values of the parameters.

Figure 3. The optimal fit of the model (smooth curve) to the particle mass concentration time series observed during the *Cigarillo #2* experiment (dots) for four particle diameter ranges. Smoking began at time $t = 0$ and lasted approximately 15 min. From the time series shown, it appears that incomplete mixing was not an issue as the model, when optimal parameters were used as input, provided good fits to the observed data. Mixing also did not appear to be an issue for the other experiments.

Figure 4. The optimal fit of the model (smooth curve) to the particle mass concentration time series observed during the *Regular Cigar #3* experiment (dots) for two particle diameter ranges. Smoking began at time $t = 0$ and lasted approximately 10 min. It appears that incomplete mixing cannot account for the observed model-measurement discrepancy, since the $0.2-0.3$ μm time series does not display the rapid decrease in concentration during the first 60 min, which

is apparent in the $0.3-0.4$ μm time series. Since the model does not take evaporation into account, it is likely that the discrepancy arises from evaporative loss (Hinds 1978; Ingebrethsen and Sears 1989).

Figure 5. The estimated size distribution of particle mass emission rate (in μg/min) and the corresponding log-normal fits for eight experiments. The text in each panel gives the type of source used in each experiment. See Table 1 for the fitted mass median diameter (MMD), geometric standard deviation (GSD), and integrated mass emissions. The average MMD and GSD were 0.20 μm and 2.3, respectively.

Figure 6. The fit of a log-normal distribution to the size distribution of mass emissions in μg/min based on the DMPS data collected for the *Regular Cigar #2* experiment. The fit shown is representative of the quality of the fits for the other two experiments where DMPS emissions estimates were obtained. All DMPS-based MMD's were near 0.2 μm and GSD's were near 1.8. The proportion of mass smaller than 0.1 μm in these fits was used as the initial guess for model optimization with the LASAIR data, which resulted in our best estimates of the size distribution of particle mass emissions (see Table 1).

Figure 7. Estimated particle deposition rates as a function of particle diameter. Each box represents the range (top and bottom limits) and median (center line) of the deposition rate across a given diameter range as determined in the present work. Dashed lines indicate results with higher associated uncertainty. The filled circles represent the results of Xu et al. (1994) for experiments when four small fans were operating at 3070 rpm, conditions similar to our own experiments.

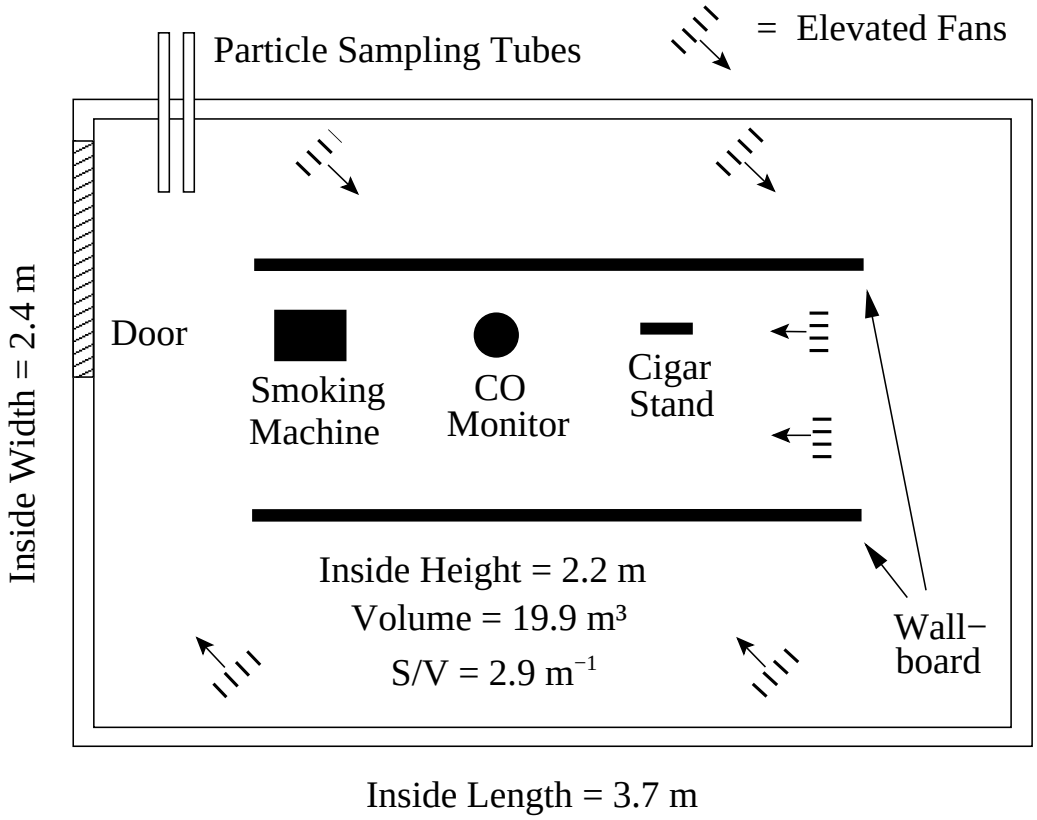
Particle Sampling Tubes
= Elevated Fans
Inside Width = 2.4 m
Door
Smoking Machine
CO Monitor
Cigar Stand
Inside Height = 2.2 m
Volume = 19.9 m³
S/V = 2.9 m⁻¹
Wall−board
Inside Length = 3.7 m

Figure 1:

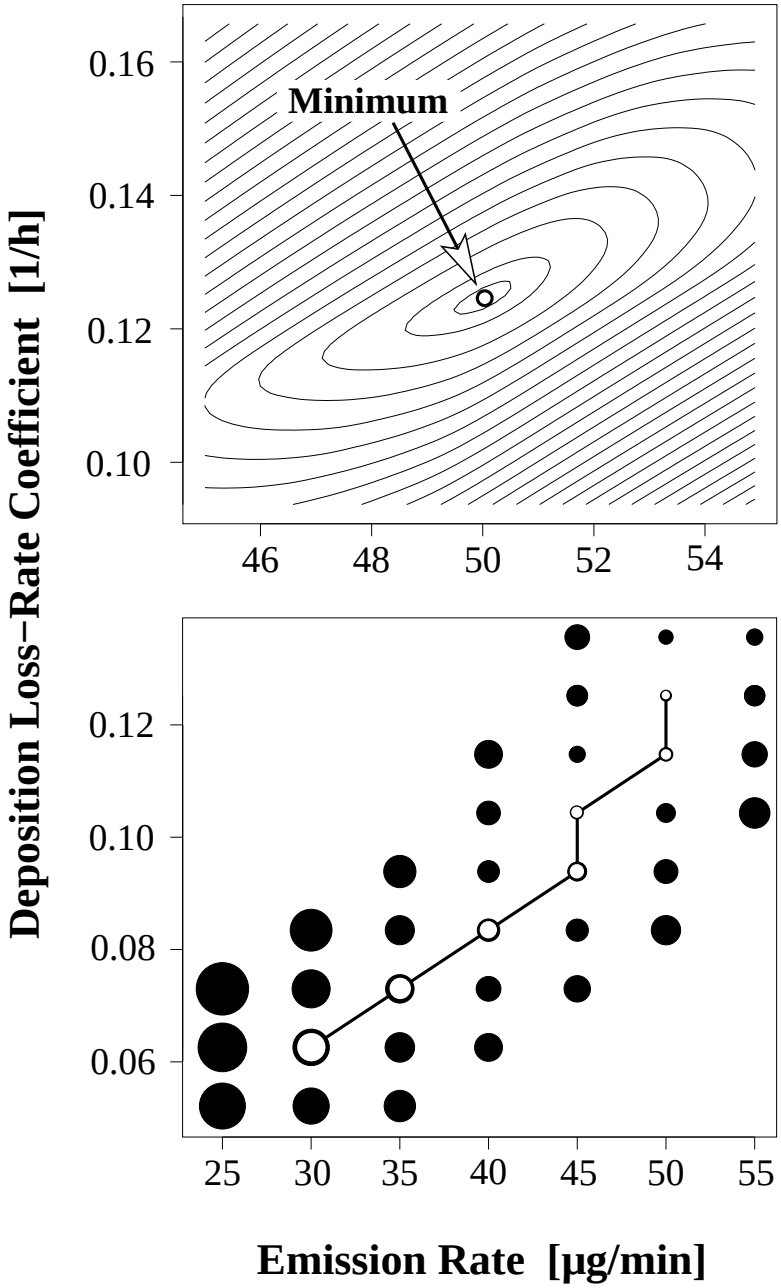
Minimum
0.16
0.14
0.12
0.10
46
48
50
52
54
0.12
0.10
0.08
0.06
25
30
35
40
45
50
55
Deposition Loss−Rate Coefficient [1/h]
Emission Rate [µg/min]

Figure 2:

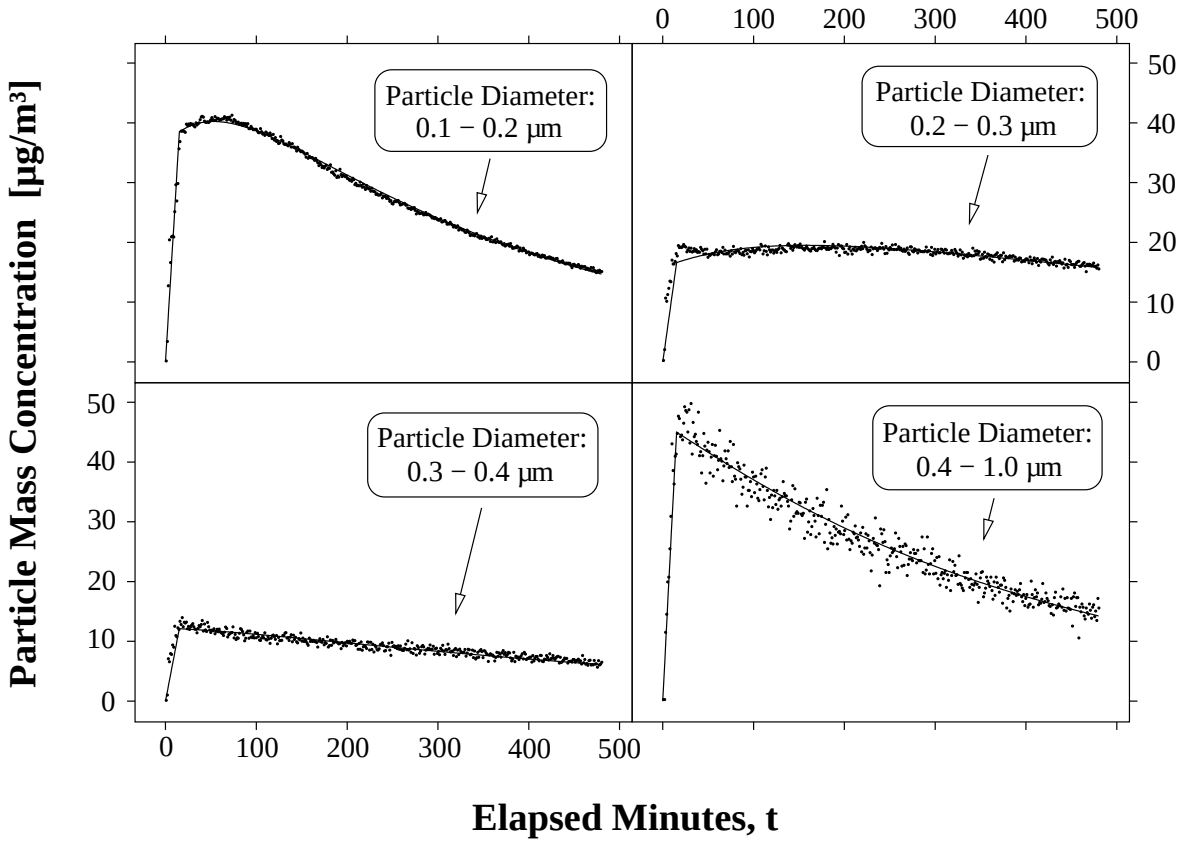
Particle Mass Concentration [µg/m³]
Particle Diameter:
0.1 − 0.2 µm
Particle Diameter:
0.2 − 0.3 µm
Particle Diameter:
0.3 − 0.4 µm
Particle Diameter:
0.4 − 1.0 µm
0
10
20
30
40
50
0
100
200
300
400
500
Elapsed Minutes, t

Figure 3:

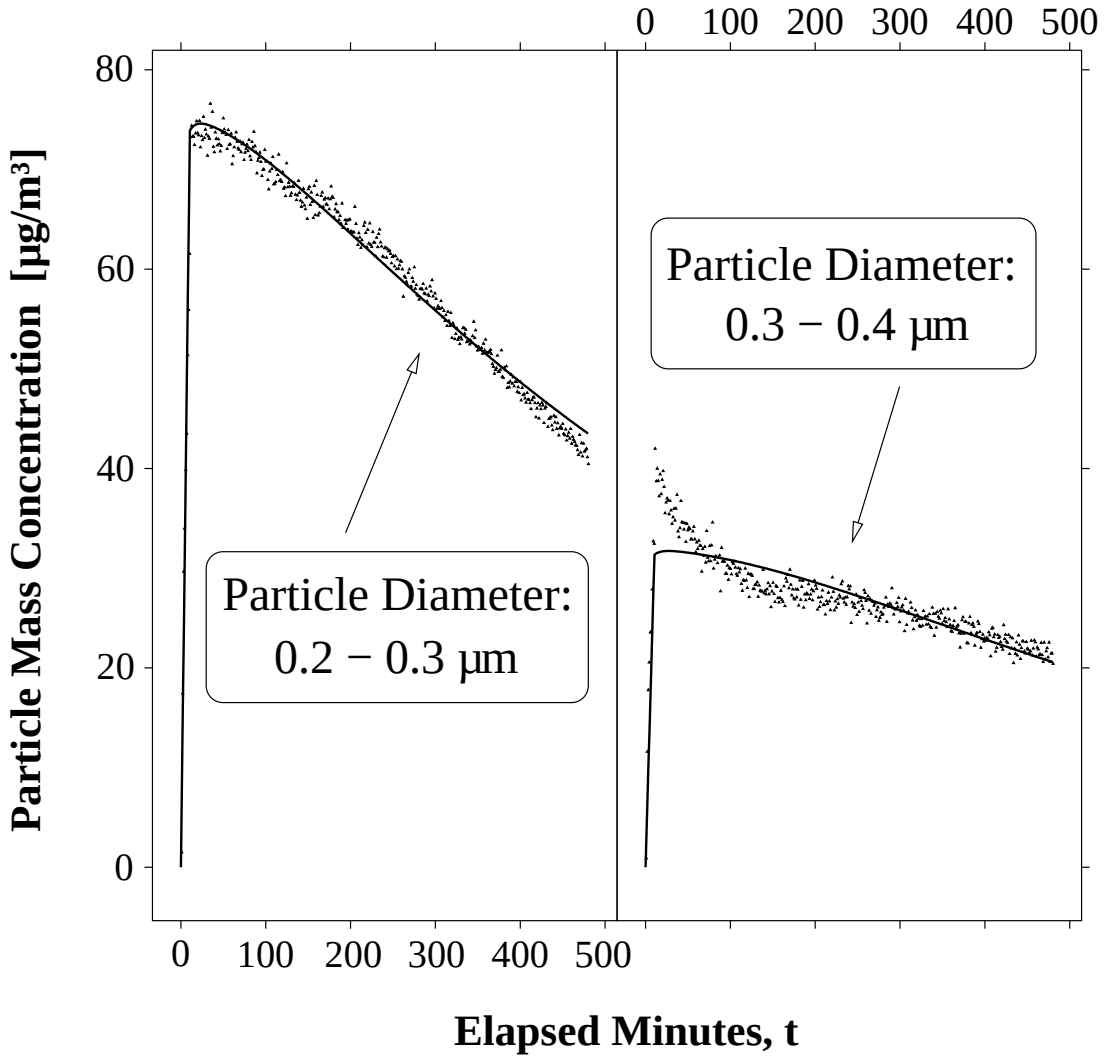
0 100 200 300 400 500
80
60
40
20
0
Particle Mass Concentration [µg/m³]
Particle Diameter:
0.3 − 0.4 µm
Particle Diameter:
0.2 − 0.3 µm
0 100 200 300 400 500
Elapsed Minutes, t

Figure 4:

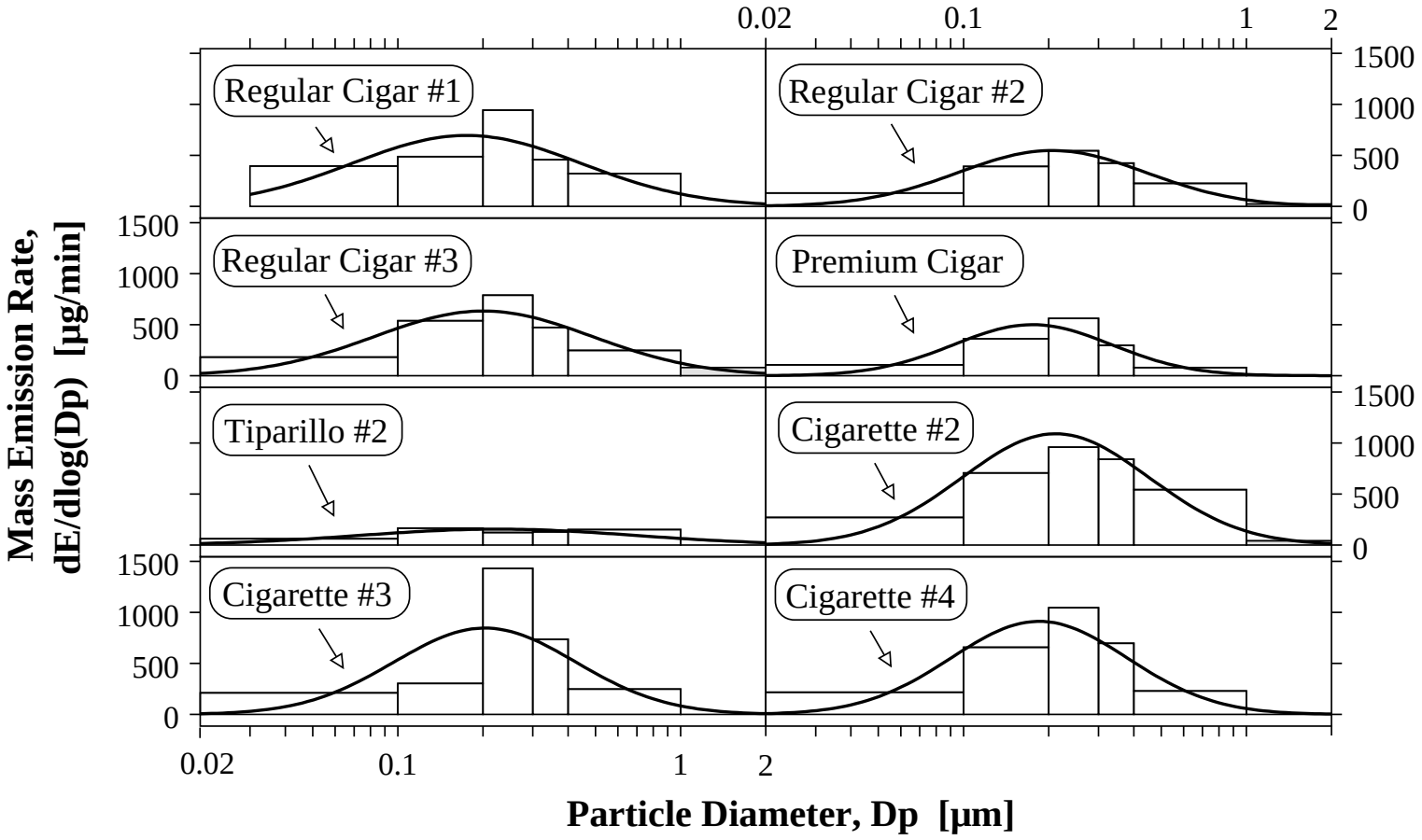
Regular Cigar #1
Regular Cigar #2
Regular Cigar #3
Premium Cigar
Tiparillo #2
Cigarette #2
Cigarette #3
Cigarette #4
0.02
0.1
1
2
0
500
1000
1500
Mass Emission Rate,
dE/dlog(Dp) [µg/min]
Particle Diameter, Dp [µm]

Figure 5:

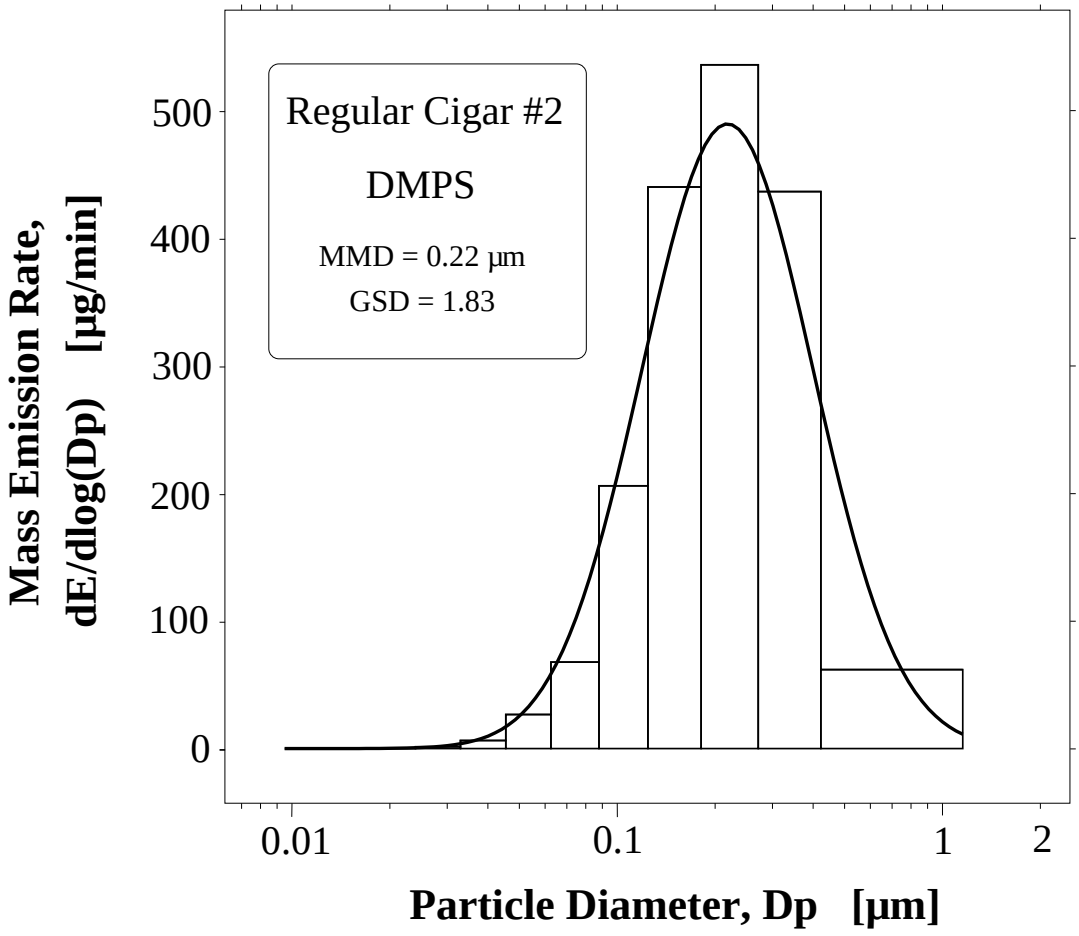
Regular Cigar #2
DMPS
MMD = 0.22 µm
GSD = 1.83
Mass Emission Rate,
dE/dlog(Dp) [µg/min]
500
400
300
200
100
0
0.01
0.1
1
2
Particle Diameter, Dp [µm]

Figure 6:

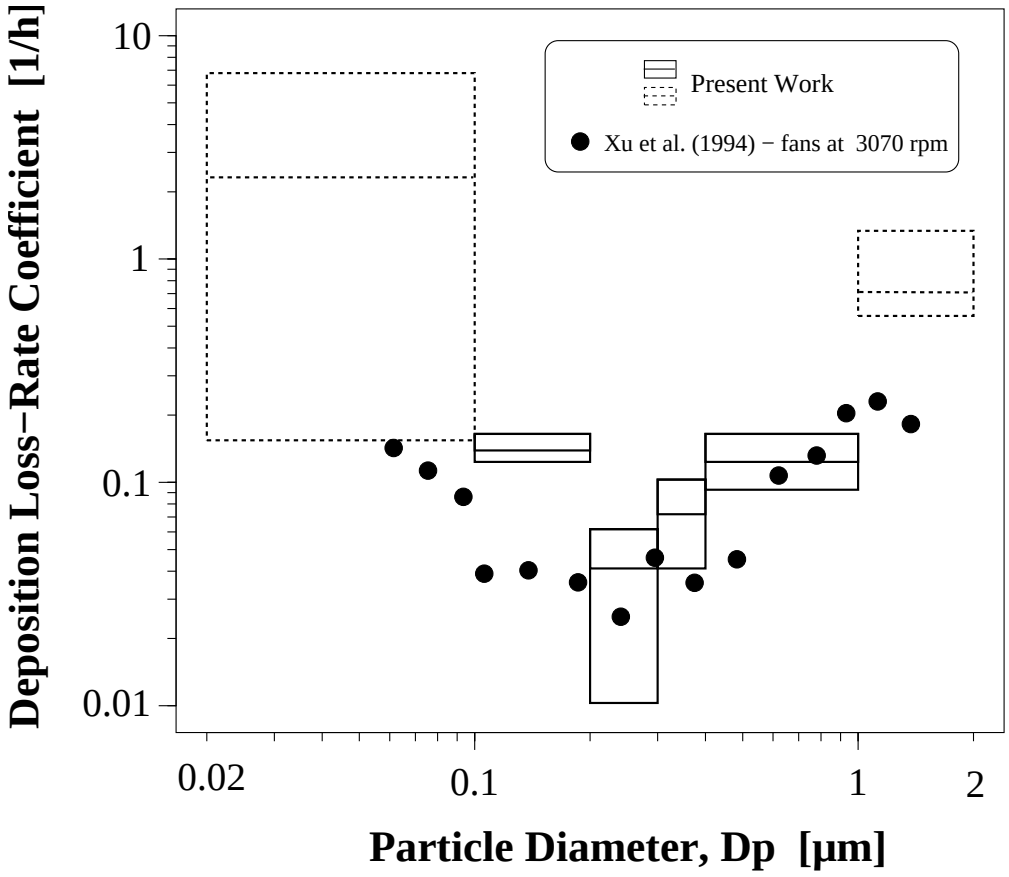
Deposition Loss−Rate Coefficient [1/h]
10
1
0.1
0.01
0.02
0.1
1
2
Particle Diameter, Dp [µm]
Present Work
Xu et al. (1994) − fans at 3070 rpm

Figure 7: